# Presynaptic Strontium Dynamics and Synaptic Transmission

Matthew A. Xu-Friedman and Wade G. Regehr
Department of Neurobiology, Harvard Medical School, Boston, Massachusetts 02115 USA

ABSTRACT   Strontium can replace calcium in triggering neurotransmitter release, although peak release is reduced and the duration of release is prolonged. Strontium has therefore become useful in probing release, but its mechanism of action is not well understood. Here we study the action of strontium at the granule cell to Purkinje cell synapse in mouse cerebellar slices. Presynaptic residual strontium levels were monitored with fluorescent indicators, which all responded to strontium (fura-2, calcium orange, fura-2FF, magnesium green, and mag-fura-5). When calcium was replaced by equimolar concentrations of strontium in the external bath, strontium and calcium both entered presynaptic terminals. Contaminating calcium was eliminated by including EGTA in the extracellular bath, or by loading parallel fibers with EGTA, enabling the actions of strontium to be studied in isolation. After a single stimulus, strontium reached higher peak free levels than did calcium (~1.7 times greater), and decayed more slowly (half-decay time 189 ms for strontium and 32 ms for calcium). These differences in calcium and strontium dynamics are likely a consequence of greater strontium permeability through calcium channels, lower affinity of the endogenous buffer for strontium, and less efficient extrusion of strontium. Measurements of presynaptic divalent levels help to explain properties of release evoked by strontium. Parallel fiber synaptic currents triggered by strontium are smaller in amplitude and longer in duration than those triggered by calcium. In both calcium and strontium, release consists of two components, one more steeply dependent on divalent levels than the other. Strontium drives both components less effectively than does calcium, suggesting that the affinities of the sensors involved in both phases of release are lower for strontium than for calcium. Thus, the larger and slower strontium transients account for the prominent slow component of release triggered by strontium.

## INTRODUCTION

Strontium is a divalent cation similar in size to calcium, which can substitute for calcium in a wide variety of biological processes. Studies at the squid giant synapse (Augustine and Eckert, 1984), the neuromuscular junction (Miledi, 1966; Dodge et al., 1969; Meiri and Rahamimoff, 1971; Mellow et al., 1982; Bain and Quastel, 1992), and at central synapses (Goda and Stevens, 1994; Abdul-Ghani et al., 1996) have shown that strontium can trigger neurotransmitter release, but that release by strontium and calcium differ in two major ways. First, the amplitude of release is reduced, indicating that strontium is less effective than calcium at triggering release. Second, in strontium, evoked release is desynchronized, such that a significant number of quanta are released for hundreds of milliseconds, compared to release triggered by calcium, which occurs primarily within a few milliseconds of stimulation.

Although the mechanism for this striking effect on the time course of release is unknown, it makes strontium a useful experimental tool. Strontium is often used to isolate individual quantal currents underlying evoked release (Oliet et al., 1996; Choi and Lovinger, 1997; Morishita and Alger, 1997; Otis et al., 1997; Behrends and ten Bruggencate, 1998; Lévénès et al., 1998). It is also a useful probe of the calcium-dependent processes involved in release. This is an important issue because calcium is known to play multiple roles in transmission. Studies of paired-pulse facilitation, posttetanic potentiation, and asynchronous release (also called delayed release) have pointed to the existence of two sensors with high and low affinity for calcium (Stanley, 1986; Delaney et al., 1989; Adler et al., 1991; Swandulla et al., 1991; Delaney and Tank, 1994; Goda and Stevens, 1994; Kamiya and Zucker, 1994; Atluri and Regehr, 1996, 1998). One study has suggested that strontium is more effective at triggering the high-affinity site than the low one (Goda and Stevens, 1994). This hypothesis has led to the use of strontium to identify candidate high-affinity calcium sensors, such as synaptotagmin III, based on its high relative strontium binding affinity (Li et al., 1995).

To more fully understand synaptic transmission in the presence of strontium, it is necessary to characterize the amplitude and time course of strontium levels in presynaptic terminals following stimulation. Because strontium is so similar to calcium, its presynaptic levels are subject to the same regulatory mechanisms during influx (Hagiwara and Ohmori, 1982; Hess et al., 1986; Mangoni et al., 1997; Wakamori et al., 1998), internal sequestration and buffering (Mermier and Hasselbach, 1976; Rasgado-Flores et al., 1987; Fujimori and Jencks, 1992a, b), and extrusion (Graf et al., 1982). However, because strontium and calcium have different kinetics and affinity in these processes, it is possible that intraterminal strontium and calcium dynamics differ.

In this paper we measure presynaptic strontium levels in the mouse cerebellar granule cell to Purkinje cell synapse.

---

This preparation offers the advantage of a simple cellular architecture, which is ideal for the measurement of changes in presynaptic calcium with fluorescent indicators (Regehr and Tank, 1991; Regehr and Atluri, 1995). Here we extend this method to the measurement of presynaptic strontium levels. We find that the slow time course of release triggered by strontium can be accounted for by the observation that stimulus-evoked changes in strontium are larger and longer-lived than are changes in calcium.

## METHODS

Transverse cerebellar slices were prepared using 11–21-day-old ICR mice (Harlan Sprague-Dawley, Indianapolis, IN), using methods similar to those described previously (Regehr and Atluri, 1995). All recordings were carried out at 24°C in one of three external solutions. Standard external solution, which is also referred to as $Ca_e$, contained (in mM) 2 $CaCl_2$, 125 NaCl, 2.5 KCl, 1 $MgCl_2$, 26 $NaHCO_3$, 1.25 $NaH_2PO_4$, and 25 glucose (310 mOsm). $Sr_e$ refers to a solution in which 2 mM $SrCl_2$ replaces $CaCl_2$. External solutions with no divalents added contained 6 $\mu$M calcium, as assessed with a calcium-sensitive electrode (Orion model 9720 BN, Beverly, MA), calibrated with a 0.1 M $CaCl_2$ standard (Orion). Sr-$EGTA_e$ refers to external solution containing 4 $SrCl_2$, 2 EGTA, 125 NaCl, 2.5 KCl, 1 $MgCl_2$, 34 $NaHCO_3$, 1.25 $NaH_2PO_4$, and 25 glucose (320 mOsm). Flow rates were at least 2 ml/min, and all solutions were bubbled with 95%/5% $O_2/CO_2$ at pH 7.4.

Parallel fibers were loaded with ion-sensitive indicators by directing a jet of the acetoxymethyl ester (AM) form (Tsien, 1981) over a restricted area of the molecular layer. Slices were incubated for another hour to allow the indicator to diffuse along the parallel fibers. The fluorescence light source was either a 150 W xenon bulb or a 100 W tungsten bulb. Fluorescence transients produced by extracellular stimulation of the fiber tract were recorded from parallel fibers in a 100-$\mu$m-diameter region in the molecular layer hundreds of microns away from the fill site. A photodiode that responded to a step change in intensity with a time constant of 900 $\mu$s was used to record the fluorescence. Signals were filtered with a 500 Hz 8-pole filter (Frequency Devices model 900, Haverhill, MA), and sampled at 5 kHz with an Instrutech ITC-16 interface. Igor Pro (Wavemetrics, Lake Oswego, OR) and Pulse Control software (Herrington and Bookman, 1995) were used to collect and analyze data.

For fura-2 (Grynkiewicz et al., 1985), mag-fura-5 (Zhao et al., 1996), and fura-2FF (London et al., 1996) we used excitation filter 380DF15, dichroic 435DRLP, and emission filter 455LP, unless otherwise noted. For magnesium green, a 450–490 nm excitation filter, a 515DRLP dichroic, and a 530LP emission filter were used. For calcium orange, a 540DF15 excitation filter, a 560DRLP dichroic, and an OG570 emission filter were used. For some fura-2 experiments, as indicated, we used a filter wheel (Sutter Lambda 10, Novato, CA) to select between a range of excitation filters (340DF15, 355DF15, 360DF15, 370DF10, and 380DF15). We also screened several other indicators (magnesium orange, calcium green-2, calcium crimson, Oregon green-5N, BTC, furaptra, Newport green), none of which was more sensitive to strontium than calcium, so we chose the five most suitable indicators listed above. Optical components were obtained from Chroma (Brattleboro, VT) and Omega Optical (Brattleboro, VT) with the exception of the magnesium green filter set, which was obtained from Zeiss. Fluorescence data are presented as percent $\Delta F/F$. For clarity, all fura-2 (with the exception of Fig. 4), mag-fura-5, and fura-2FF traces are inverted such that an increase in calcium corresponds to an increase in $\Delta F/F$.

We recorded excitatory postsynaptic currents (EPSCs) from Purkinje cells in the whole-cell patch configuration at a holding potential of $-70$ mV. The internal solution consisted of (in mM) 108.5 $CsSO_4$, 10 EGTA, 4 $CaCl_2$, 10 HEPES, 1.5 $MgCl_2$, 5.35 $MgSO_4$, 4 NaATP, and 0.1 D-600 (pH 7.5, 317 mOsm). Electrode resistances were 1–1.5 M$\Omega$. Bicuculline (20 $\mu$M) was added to the external solutions to suppress inhibitory postsyn-aptic currents mediated by $GABA_A$ receptors. Parallel fibers were stimulated extracellularly with a second electrode. In experiments in which we measured spontaneous miniature EPSCs (mEPSCs), TTX (0.25 $\mu$M) was added to the external solutions.

To prevent de-esterification, EGTA-AM solutions were prepared immediately before use. As described in Atluri and Regehr (1996), introduction of this slow calcium buffer accelerates the decay of calcium in parallel fibers without greatly affecting the peak influx.

With the exception of fura-2FF (Teflabs, Austin, TX), all fluorescent indicators and EGTA-AM were obtained from Molecular Probes (Eugene, OR). Other chemicals were obtained from SIGMA (St. Louis, MO).

## Calibration of divalent-sensitive indicators

The binding affinities of calcium-sensitive indicators for strontium and calcium were determined with the method described by Tsien (1980). Briefly, divalent levels are buffered to known levels with EGTA, while minimizing calcium contamination from glassware, chemicals, and the distilled water supply. Calibration solutions contained 100 mM KCl, 10 mM MOPS, and 1 $\mu$M indicator in addition to EGTA and divalents, as described below. We verified the pH of all solutions using a Fisher Accumet model 15, calibrated using National Institute of Standards and Technology recipes, adjusting solutions to pH 7.20 $\pm$ 0.02 after all ingredients were added. We calculated the divalent binding affinities of EGTA using the tables in Martell and Smith (1974), as explained in Tsien and Pozzan (1989) (see footnote to their Table 1). The binding affinity of EGTA for calcium and strontium depends on ionic strength, temperature, and pH (roughly doubling for a 0.15 increase in pH). Under our conditions, the $K_d$ of EGTA is 150.5 nM for calcium, 43.65 $\mu$M for strontium, and 19.7 mM for magnesium.

Following Tsien and Pozzan (1989), we prepared two calibration solutions in our MOPS buffer, one with 10 mM EGTA ("0 CaEGTA"), and one with 10 mM of both EGTA and calcium ("10 CaEGTA"). The amount of calcium in the 10 CaEGTA solution was carefully titrated to match the concentration of EGTA using the pH-metric method (Moisescu and Pusch, 1975). Starting with 0 CaEGTA in a quartz cuvette, we performed serial dilutions with the 10 CaEGTA solution to raise the total concentration of calcium in the cuvette to (in mM) 0, 1, 2, 3, 4, 5, 6, 7, 8, 8.5, 9, 9.25, 9.5, 9.75, and 10, which corresponds to free calcium of (in nM) 0, 16.7, 37.6, 64.5, 100, 150, 226, 351, 602, 852, and (in $\mu$M) 1.32, 1.85, 2.84, 5.73, and 38.7, respectively. We prepared a similar series for strontium using 0 SrEGTA and 10 SrEGTA solutions, setting the total strontium concentration to (in mM) 0, 0.25, 0.5, 0.75, 1, 1.5, 2, 3, 4, 5, 6, 7, 8, 9, and 10; corresponding to calculated free strontium concentrations of (in $\mu$M) 0, 1.11, 2.29, 3.52, 4.82, 7.64, 10.8, 18.5, 28.8, 42.9, 63.8, 97.3, 159, 294, and 639.

For the low-affinity indicators (magnesium green, mag-fura-5, fura-2FF), the EGTA buffered series was used to set values of calcium up to 38.7 $\mu$M. Higher values of calcium and strontium were required to allow a good estimate of the dissociation constants. Therefore, we added a further series with 0 $\mu$M $CaCl_2$ ("0 Ca"), 100 $\mu$M $CaCl_2$ ("100 Ca"), and 1000 $\mu$M $CaCl_2$ ("1000 Ca"), in our MOPS buffer. Starting with the 0 Ca solution, we performed serial dilutions, first with 100 Ca solution, and then with the 1000 Ca solution, covering a free calcium concentration of (in $\mu$M) 10, 20, 30, 50, 75, 100, 200, 300, and 1000. The actual free calcium concentration departs from this for two reasons. First, we estimate that ~2 $\mu$M calcium was present in our nominally 0 Ca solution, as assessed with a calcium-sensitive electrode; therefore, this series could not be used for calcium concentrations lower than 10 $\mu$M. Second, calcium bound to 1 $\mu$M of the indicator itself reduces free calcium in the above dilution series to (in $\mu$M) 9.3, 19.2, 29.1, etc., for a 5 $\mu$M $K_d$ indicator, and to 9.7, 19.5, 29.4, etc., for a 20 $\mu$M $K_d$ indicator. It was also necessary to measure fluorescence at higher strontium levels than those achieved with the EGTA-buffered series. This was done by adding 1 M $SrCl_2$.

A SPEX fluorolog (Edison, NJ) was used to measure fluorescence spectra. Spectra were determined for magnesium green with 475 nm excitation and 490–650 nm emission; for calcium orange excitation was

530 nm and emission 540–660 nm; for fura-2 and fura-2FF excitation was 250–450 nm and emission 510 nm; and for mag-fura-5 excitation was 250–450 nm and emission 490 nm. There were small shifts in some of the spectra, including the isosbestic point shift displayed by fura-2 in Fig. 4. There were only slight differences in the peak fluorescence values measured in saturating concentrations of strontium versus calcium. Thus, for the wavelengths we employed in our experiments, such small alterations in the excitation and emission spectra for strontium compared to calcium are unlikely to contribute significantly to the differences seen in the fluorescence transients measured in strontium compared to those measured in calcium. Dissociation constants were determined using the following wavelengths: 530 nm emission for magnesium green, 572 nm emission for calcium orange, and 380 nm excitation for fura-2, mag-fura-5, and fura-2FF. Fluorescence values were fit to an equation of the form,

$$F = \frac{F_{max}[\text{divalent}] + F_{min}K_d}{[\text{divalent}] + K_d}.$$

For low divalent concentrations, fluorescence is $F_{min}$, and for saturating divalent concentrations, fluorescence is $F_{max}$. For the wavelengths we used, an increase in divalent levels led to a decrease in fluorescence for fura-2, mag-fura-5, and fura-2FF, and to an increase in fluorescence for magnesium green and calcium orange. For the purpose of presentation in Fig. 1 A, calibration curves have been normalized to range between 0 (no divalent bound to the fluorophore) and 1 (saturating divalent levels). As shown in Fig. 1 B and Table 1, these indicators differ greatly in their relative sensitivity to calcium and strontium. For example, fura-2 is 33 times more sensitive to calcium than to strontium, compared to 3.5 times
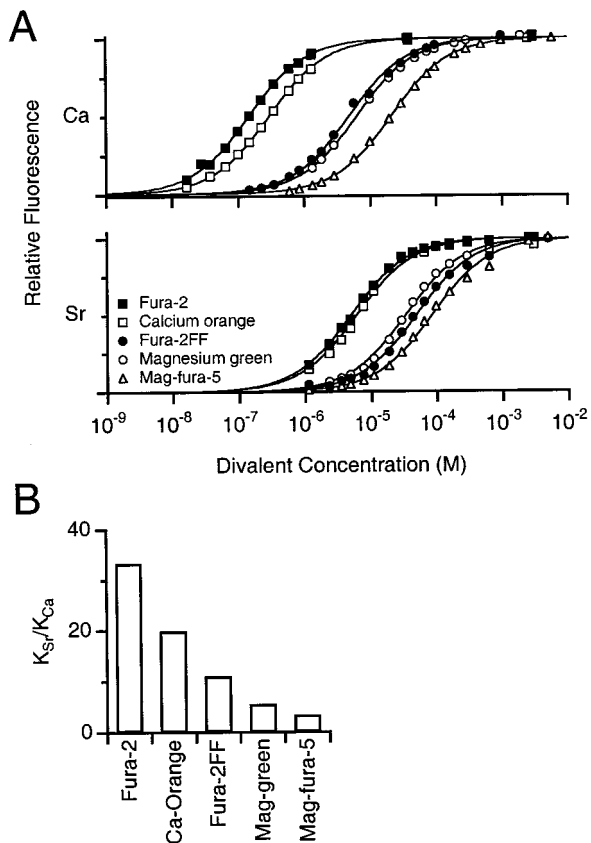


FIGURE 1  Responses of different indicators to calcium and strontium. (A) Binding affinity curves for different indicators for calcium (*top graph*) and strontium (*bottom graph*). Curves were measured and normalized as described in Methods. Measured $K_d$ values are found in Table 1. (B) Measured $K_d$ ratios for different indicators, from data in (A).
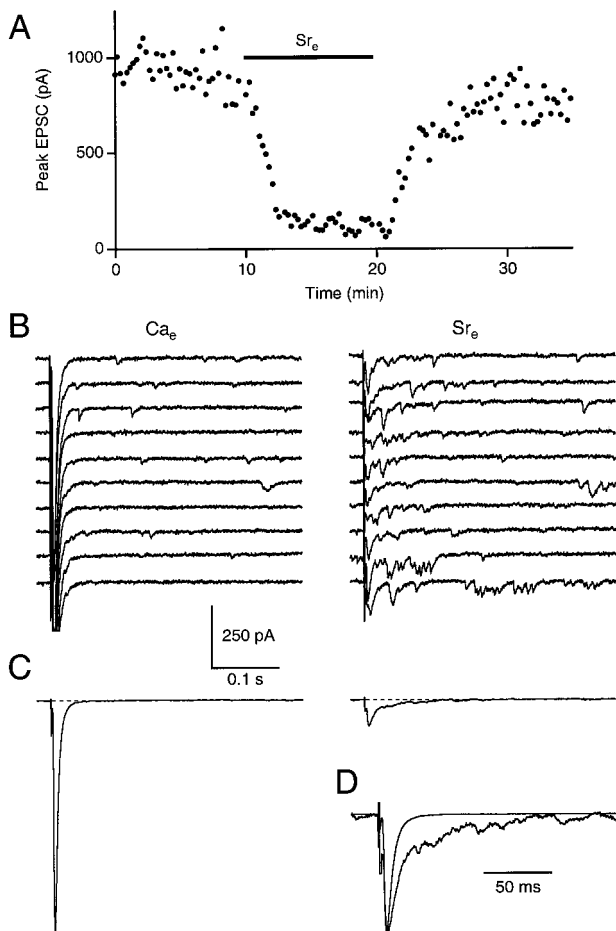
**TABLE 1  Dissociation constants measured in 0.1 M KCl, 10 mM MOPS, pH 7.2, room temperature**

| Indicator | $K_{Ca}$ ($\mu$M) | $K_{Sr}$ ($\mu$M) |
|---|---|---|
| Fura-2 | 0.15 | 5 |
| Calcium orange | 0.30 | 6 |
| Magnesium green | 6 | 33 |
| Mag-fura-5 | 20 | 70 |
| Fura-2FF | 5 | 55 |

for mag-fura-5. All calcium binding affinities measured here are close to previously reported values, except for the new dye fura-2FF, which has been reported by the manufacturer to have a $K_{Ca}$ of 35 $\mu$M.

Fluorescence signals may be contaminated by presynaptic magnesium levels, particularly with magnesium green and mag-fura-5, which bind magnesium with dissociation constants of 1 mM and 2.3 mM, respectively. We confirmed the magnesium dissociation constant for mag-fura-5 under our experimental conditions using the method described by Tsien (1980). We also attempted to measure the dissociation constant for magnesium binding to fura-2FF. We found that fura-2FF did not respond to magnesium changes that were <1 M, indicating that fura-2FF has negligible magnesium affinity.

## Modeling

A single-compartment model was made for fluorescence and divalent transients. The model incorporated an endogenous buffer (concentration 2 mM, $K_{d\text{-}Ca}$ 20 $\mu$M, $K_{d\text{-}Sr}$ 30 $\mu$M, on rate $2 \cdot 10^8$ M$^{-1}$ s$^{-1}$), a divalent-sensitive indicator (concentration 3 $\mu$M, $K_d$ values in Table 1, on rate $5 \cdot 10^8$ M$^{-1}$ s$^{-1}$), a Michaelis-Menten pump ($V_{max}/K_p$ for calcium 2000 s$^{-1}$, for strontium 400 s$^{-1}$), differential influx (calcium 45 $\mu$M, strontium 48 $\mu$M, and up to a 4.5 $\mu$M increase in intracellular calcium accompanying strontium influx), and leak to provide a resting calcium of 50 nM. These model parameters were chosen by fitting the signals measured using low-affinity indicators. The simple pump here does not perfectly capture the time course of calcium decay, but it is useful as a first approximation.

## RESULTS

Replacing calcium with strontium in the external solution strongly affects the amplitude and time course of evoked synaptic release in the granule cell to Purkinje cell synapse in mouse cerebellum, in a manner similar to that observed at other synapses (Fig. 2). The peak EPSC drops ~10-fold when the external solution is switched from a solution containing 2 mM calcium (Ca$_e$) to one containing 2 mM strontium (Sr$_e$) (Fig. 2, A and C). In Ca$_e$, there are very few release events 25 ms after the stimulus, whereas in Sr$_e$, a significant amount of release persists for hundreds of milliseconds (Fig. 2 B). The persistent release in Sr$_e$ is also evident in the average EPSC (Fig. 2 D).

## Measuring the time course of strontium decay in the presynaptic terminal

To explore the effect of strontium on neurotransmitter release, we measured changes in presynaptic intracellular residual free strontium levels ($\Delta[\text{Sr}]_i$) in Sr$_e$, using an approach that we have used previously to measure presynaptic residual intracellular free calcium levels ($\Delta[\text{Ca}]_i$). Granule

FIGURE 2 Effect of strontium on Purkinje cell EPSCs. (*A*) EPSC peak amplitude drops when the external solution is changed from $Ca_e$ to $Sr_e$. Each circle represents the peak EPSC in response to a single stimulation of the parallel fibers. (*B*) Sample EPSCs recorded in $Ca_e$ or $Sr_e$. Each sweep represents the response to a stimulus in the molecular layer (stimulus artifact edited for clarity). Traces are expanded to show mEPSCs, so EPSCs in $Ca_e$ are truncated. (*C*) Average EPSCs recorded in $Ca_e$ ($n = 38$ traces) or $Sr_e$ ($n = 17$). (*D*) Average EPSCs from (*C*) scaled and overlaid.

cell terminals are small ($\sim 1$ $\mu$m diameter) and represent $\sim 85\%$ of the total granule cell axon volume (Palay and Chan-Palay, 1974). Therefore, calcium reaches spatial equilibrium quickly, and $\Delta F/F$ measurements reflect divalent levels in presynaptic terminals.

Despite screening many indicators (see Methods), we did not find an indicator that was selective for strontium over calcium. However, we found a number that responded to both strontium and calcium, but with differential sensitivities. We began by using mag-fura-5, magnesium green, and fura-2FF, which all bind calcium and strontium with low affinity. As shown in Fig. 3 *A* for mag-fura-5, changing from $Ca_e$ to $Sr_e$ decreased the amplitude and slowed the time course of the $\Delta F/F$ signal. Similar effects were reported by all of the low-affinity indicators, but the reduction in peak $\Delta F/F$ depended on the indicator: the ratio of peak $\Delta F/F$ signals in $Sr_e$ compared to $Ca_e$ for single pulses was $32 \pm 2\%$ (mean $\pm$ SE, $n = 6$) for magnesium green, $51 \pm$

$2\%$ ($n = 9$) for mag-fura-5, and $22 \pm 1\%$ ($n = 4$) for fura-2FF.

When combined with the measured dissociation constants of the different indicators for strontium and calcium, these experiments allow us to estimate the relative amplitudes of $\Delta[Sr]_i$ in $Sr_e$ and $\Delta[Ca]_i$ in $Ca_e$. Assuming that the $\Delta F/F$ signals in $Sr_e$ result exclusively from an increase in strontium, the ratio of the amplitude of $\Delta[Sr]_i$ in $Sr_e$ to the amplitude of $\Delta[Ca]_i$ in $Ca_e$ ($R_{Sr/Ca}$) can be estimated for these low-affinity indicators by the formula,

$$R_{Sr/Ca} = \frac{\Delta[Sr]_i}{\Delta[Ca]_i} = \left(\frac{K_{Sr}}{K_{Ca}}\right)\left(\frac{(\Delta F/F)_{Sr}}{(\Delta F/F)_{Ca}}\right), \quad (1)$$

where $K_{Sr}$ and $K_{Ca}$ are the dissociation constants for indicator binding to strontium and calcium, respectively. $K_{Sr}/K_{Ca}$ is 3.5 for mag-fura-5, 5.5 for magnesium green, and 11 for fura-2FF. $R_{Sr/Ca}$ is estimated to be $1.68 \pm 0.07$ for mag-fura-5, $1.74 \pm 0.11$ for magnesium green, and $2.18 \pm 0.07$ for fura-2FF.

We also examined $\Delta F/F$ signals for fura-2 and calcium orange, which are useful in this study because of their relative insensitivity to magnesium and their high sensitivity to calcium relative to strontium ($K_{Sr}/K_{Ca}$ is 33 for fura-2 and 20 for calcium orange). As has been shown previously, the presynaptic calcium transient produced by a single stimulus is sufficiently large to partially saturate fura-2, thereby distorting calcium signals in two ways: the $\Delta F/F$ signal is slower than that measured with low-affinity indicators, and the amplitude is a nonlinear function of the free divalent levels. Thus, the second of two closely spaced stimuli (10 ms) results in an incremental $\Delta F/F$ signal that is much smaller than that produced by the first stimulus (Fig. 3 *Bb*), even though experiments using low-affinity indicators show that the additional influx is identical. Changing from $Ca_e$ to $Sr_e$ decreased the degree of saturation and the amplitude of the fura-2 $\Delta F/F$ signal. The peak height of the single pulse dropped to $27.6 \pm 1.7\%$ ($n = 15$). The ratio of the height of a double pulse to a single pulse ($R_{21}$) was $1.29 \pm 0.01$ ($n = 15$) in $Ca_e$ and $1.66 \pm 0.02$ ($n = 15$) in $Sr_e$. The higher $R_{21}$ indicates that fura-2 is less, but still partially, saturated in $Sr_e$ compared to $Ca_e$, which is qualitatively consistent with the lower affinity of fura-2 for strontium. Similar results were obtained with calcium orange (peak height $32.1 \pm 2.8\%$, $R_{21}$ in calcium $1.37 \pm 0.004$, $R_{21}$ in strontium $1.67 \pm 0.05$, $n = 9$).

The slowing of the time course in $Sr_e$ that was revealed by the low-affinity indicators (Fig. 3 *Ac*) was not apparent when fura-2 was used (Fig. 3 *Bc*). Because of indicator saturation, high-affinity indicators provide a poor estimate of the time course of the underlying free calcium and strontium levels (Konishi et al., 1991; Regehr and Atluri, 1995; Atluri and Regehr, 1996; Zhao et al., 1996). However, the degree of saturation of calcium orange and fura-2 can be used to estimate peak $\Delta[Ca]_i$ and $\Delta[Sr]_i$ (Regehr and Atluri, 1995; Sabatini and Regehr, 1995), yielding estimates of $R_{Sr/Ca}$ of $\sim 7$. This value is considerably higher than for
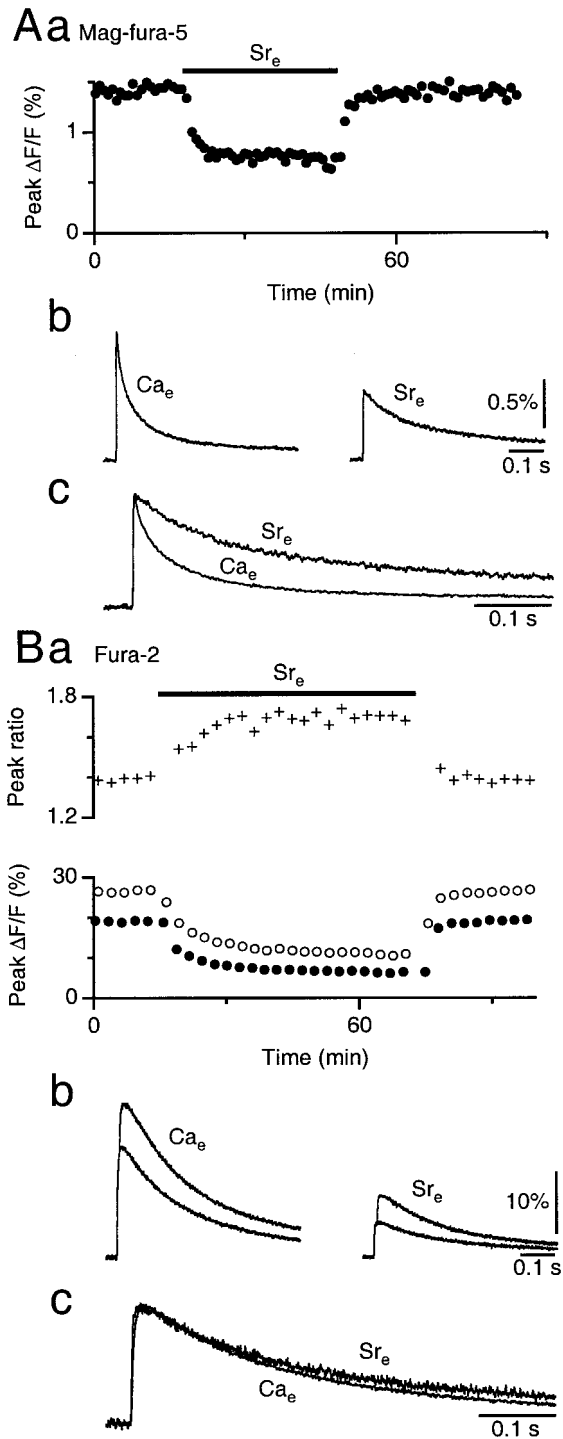
FIGURE 3   Effect of strontium on fluorescence transients measured with the low-affinity indicator mag-fura-5 (A) and the high-affinity indicator fura-2 (B). (Aa) Peak $\Delta F/F$ during application of $Sr_e$. Each circle represents the peak $\Delta F/F$ in response to single parallel fiber stimulation. (b) Average $\Delta F/F$ transients recorded in $Ca_e$ or $Sr_e$. (c) Average $\Delta F/F$ transients from b scaled and overlaid. (Ba) Peak $\Delta F/F$ for fura-2 in response to single and double pulse stimuli (bottom). Filled circles represent the peak $\Delta F/F$ in response to single stimulation of the parallel fibers, and open circles represent the peak $\Delta F/F$ in response to two stimuli, spaced 10 ms apart. In the top part, plus signs represent the ratio of peak $\Delta F/F$ to double stimuli over single stimuli. (b) Average $\Delta F/F$ transients in response to single and double pulse stimuli recorded in $Ca_e$ or $Sr_e$. (c) Average single pulse $\Delta F/F$ transients from b scaled and overlaid.

low-affinity indicators (1.7–2.2). One possible explanation is that signals detected by these indicators in $Sr_e$ might be contaminated by calcium. Fura-2 and calcium orange would be more sensitive to such contamination because of their selectivity for calcium over strontium binding.

## Using fura-2 to separate calcium and strontium signals

We used fura-2 to distinguish between strontium and calcium transients, and to determine whether strontium makes a major contribution to the fluorescence signals in $Sr_e$. We found that the shift of the excitation spectrum of fura-2, which is a well-known property of fura-2 binding to calcium, has a different wavelength dependence for strontium and calcium (Fig. 4 A): the isosbestic point for fura-2 is 357 nm for calcium and 363 nm for strontium (Fig. 4 A). Thus a change in calcium levels will not alter the fluorescence intensity for 357-nm excitation, while a change in strontium levels will not alter the intensity for 363-nm excitation. Such a shift in the isosbestic point has been observed and exploited for fura-2 binding to other divalents (e.g., Sage et al., 1989; Murray and Kotlikoff, 1991; Vega et al., 1994), and we also take advantage of it here. For both $Sr_e$ and $Ca_e$ the stimulus-induced fluorescence increased for 340-nm excitation (Fig. 4 B, bottom) and decreased for 380-nm excitation (Fig. 4 B, top). But for an excitation filter centered at 355 nm, fluorescence decreased in $Ca_e$ but increased in $Sr_e$ (Fig. 4 B, middle). The reversal in the direction of the $\Delta F/F$ signal for the 355-nm filter can only be explained if fura-2 is binding a different ion with a different isosbestic point, which in this case indicates a significant influx of strontium in $Sr_e$. Thus strontium makes a major contribution to the fluorescence transient measured in $Sr_e$, even though fura-2 is much more sensitive to calcium than to strontium. The possibility remains, however, that calcium also contributes to the signal.

## Elimination of calcium contamination

We used EGTA to determine whether calcium contributes to the fluorescence transient in $Sr_e$. Because EGTA binds calcium with an affinity 300 times greater than that of strontium (Martell and Smith, 1974), it is possible to perturb the calcium transient without greatly affecting the strontium transient. EGTA is commonly used to manipulate the magnitude and time course of calcium transients (e.g., Adler et al., 1991; Swandulla et al., 1991; Atluri and Regehr, 1996; Feller et al., 1996). As shown in Fig. 5 A, after bathing the slices in 20 $\mu$M EGTA-AM for 10 min, EGTA-AM enters the presynaptic terminal where it is deesterified into EGTA, leading to an acceleration of the decay of the calcium transient reported by magnesium green, with only a modest drop in amplitude (Fig. 5 Aa, b). These effects are readily explained by the slow on-rate of calcium binding to EGTA (Smith et al., 1984). By making the calcium contribution
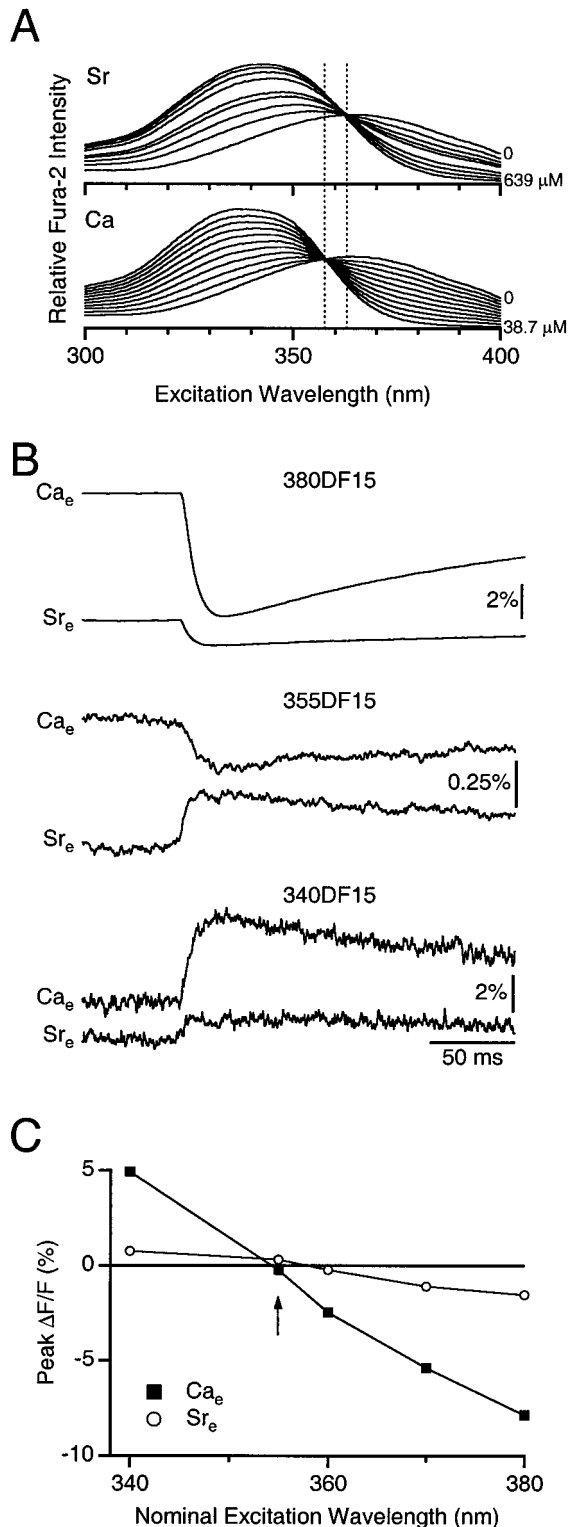
distinctively rapid, high concentrations of EGTA inside the cell allow separation of strontium and calcium transients. When the external solution is changed to $Sr_e$, two components are revealed in the $\Delta F/F$ signal (Fig. 5 $Ac$): a fast decaying component that roughly matches the shape of the early calcium transient and a slowly decaying component.

Similarly, if we apply EGTA-AM after switching to $Sr_e$, the $\Delta F/F$ signal shows an early fast component and a later slow component (Fig. 5 $Bb$, $c$). During the first 100–200 ms, there is a significant difference between the $Sr_e$ and $Sr_e$+EGTA-AM transients, which corresponds to the duration of the signal in $Ca_e$ (Fig. 5 $Bb$). These results suggest that the fast component that emerges after treatment with EGTA-AM is largely due to calcium contamination. Part of the signal may arise from calcium contamination of the external solution. Using a calcium-sensitive electrode, we found that the external solution with no added divalents had 6 $\mu M$ free calcium, similar to previously reported values (Bers, 1982; Miller and Smith, 1984). Another important factor may be our inability to lower external calcium levels deep within the brain slice.

To address these issues and eliminate calcium contamination, we used EGTA in the external solution. $Sr$-EGTA$_e$ contains 2 mM EGTA and 4 mM $SrCl_2$. We calculate that with this external solution, even if there was an initial contamination of 20 $\mu M$ calcium in the external solution, the inclusion of EGTA would reduce external calcium levels to below 100 nM. The remainder of the EGTA binds strontium, leaving 2 mM free strontium. In this solution the sharp peak observed after loading with EGTA-AM is nearly eliminated (Fig. 6, $A$ and $C$). If we subtract the fluorescence transient recorded in $Sr$-EGTA$_e$ from that recorded in $Sr_e$, the difference has a very similar time course to the transient recorded in $Ca_e$, after treatment with EGTA-AM (Fig. 6 $D$). Thus, it appears that the rapid transient component observed in $Sr_e$ after loading with EGTA-AM is a result of calcium contamination in the external solution, and that this component is eliminated in $Sr$-EGTA$_e$.

The effects of $Sr_e$ and $Sr$-EGTA$_e$ are compared for a number of calcium-sensitive indicators in Fig. 7. All show differences in peak fluorescence and time course in $Sr_e$ compared to $Sr$-EGTA$_e$. Furthermore, all indicators show

FIGURE 4  Effect of strontium on fluorescence transients measured with the high-affinity indicator fura-2. For the purposes of this figure only, fura-2 transients are shown unrectified. (A) Shift in excitation spectrum with addition of strontium or calcium. Note that the isosbestic point for calcium (357 nm) is different from the isosbestic point for strontium (363 nm). (B) Effect of excitation wavelength on average $\Delta F/F$ transients recorded in $Ca_e$ or $Sr_e$. With a 380 nm excitation filter (top traces), both calcium and strontium show a decrease in fluorescence, indicating that the effective excitation wavelength is longer than the isosbestic point for both

ions. With a 355-nm excitation filter (middle traces), the calcium transients are negative-going, indicating that the effective excitation wavelength is longer than the isosbestic point for calcium, whereas the strontium transients are positive-going, indicating the effective excitation wavelength is shorter than the isosbestic point for strontium. With the 340-nm excitation filter, both calcium and strontium show an increase in fluorescence, indicating that the effective excitation wavelength is shorter than the isosbestic point for both ions. Traces are averages of 7 to 15 trials. (C) Peak $\Delta F/F$ for calcium and strontium over a range of different excitation filters. Calcium crosses to negative transients between excitation filters of 340 and 355 nm. Strontium crosses to negative transients between excitation filters of 355- and 360-nm center wavelength (arrow). Note that the apparent crossover points differ from the isosbestic points in (A), because the optics in the microscope additionally filter the excitation light.

FIGURE 5 Calcium contamination of strontium signal, uncovered using EGTA-AM. (*A*) EGTA-AM applied in Ca$_e$. (*a*) Peak magnesium green $\Delta F/F$ measurements during the experiment. Each circle represents the peak $\Delta F/F$ in response to one stimulation of the parallel fibers. (*b*) $\Delta F/F$ signals recorded in Ca$_e$, after EGTA-AM is applied, and in Sr$_e$. (*c*) Sr$_e$ and Ca+EGTA-AM traces scaled and superimposed to show that the strontium transient initially decays very sharply, similar to the decay of the Ca+EGTA-AM transient. (*B*) EGTA-AM applied in Sr$_e$, in a different experiment from (*A*). (*a*) Peak $\Delta F/F$ measurements during the experiment. (*b*) $\Delta F/F$ signals recorded in Ca$_e$, in Sr$_e$, and after EGTA-AM is applied. (*c*) Sr$_e$ and Sr + EGTA-AM traces enlarged. After EGTA-AM is applied, a sharp initial peak becomes apparent. Traces in *b* and *c* are averages of 5 to 20 trials.
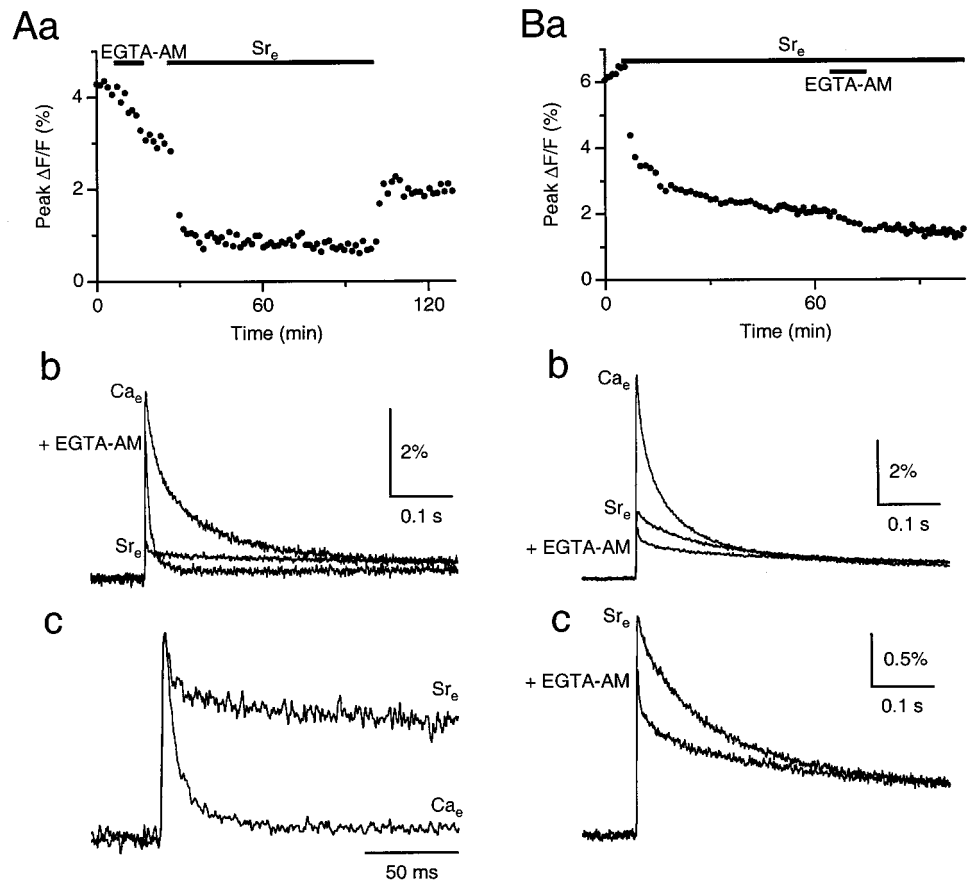
longer wash-in times in Sr$_e$ compared to Sr-EGTA$_e$ (Fig. 7, *left*), consistent with the idea that in Sr$_e$, external calcium levels in the slice are poorly controlled and that calcium is removed from the slice gradually and incompletely. The effects of Sr-EGTA$_e$ reach steady-state rapidly and wash out reliably, indicating that it is much more effective at controlling external calcium levels and better suited to estimating the relative entry of strontium and calcium. Peak $\Delta F/F$ signals and estimates of $R_{Sr/Ca}$ are smaller in Sr-EGTA$_e$ than in Sr$_e$ for all of the indicators (Fig. 7 *D*), which is consistent with calcium contamination of the signals in Sr$_e$. Furthermore, the drop in peak $\Delta F/F$ in Sr-EGTA$_e$ is more pronounced for indicators relatively less sensitive to strontium, being 21% for fura-2FF, 9% for magnesium green, and 7% for mag-fura-5. In Sr-EGTA$_e$ estimates of $R_{Sr/Ca}$ are 1.89 ± 0.02 (*n* = 6) for fura-2FF, 1.58 ± 0.05 (*n* = 9) for magnesium green, and 1.56 ± 0.11 (*n* = 4) for mag-fura-5.

We also compared the effects of Sr$_e$ and Sr-EGTA$_e$ for high-affinity calcium-sensitive indicators (Fig. 8). For both fura-2 and calcium orange, wash-in times were much longer for Sr$_e$ than for Sr-EGTA$_e$ (Fig. 8, *Aa, Ba*). Peak $\Delta F/F$ signals are smaller in Sr-EGTA$_e$ than in Sr$_e$ (Fig. 8, *Aa–c*), and ratios of fluorescence changes produced by double stimuli to those produced by single stimuli ($R_{21}$) are larger (Fig. 8 *Aa, top graph*). Signals in Sr-EGTA$_e$ do not have the rounded appearance that is characteristic of signals recorded in Ca$_e$ and Sr$_e$ (Fig. 8 *Ac*). The amplitude differences and

even the shape of the $\Delta F/F$ signals can be recreated in simulations based on a single compartment model (Fig. 8 *Ad*; see Methods). Similar results were obtained for calcium orange (Fig. 8 *B*); thus the $\Delta F/F$ signals measured with fura-2 and calcium orange are consistent with the amplitude and time course of $\Delta[Sr]_i$ estimated using the low-affinity indicators.

## Estimates of the amplitude and time course of strontium and calcium transients

Low-affinity indicators, which have fast kinetics and are not prone to saturation, were used to measure presynaptic calcium and strontium dynamics. The time courses of $\Delta[Ca]_i$ and $\Delta[Sr]_i$ appear to be reflected accurately by the time courses of the fluorescence changes of low-affinity indicators. We corrected the $\Delta F/F$ transient measured in Sr-EGTA$_e$ using Eq. 1 to estimate relative $\Delta[Sr]_i$. Initial time course estimates were based on measurements with magnesium green, which provided the best signal-to-noise ratio. The average time course and relative amplitude of $\Delta[Ca]_i$ and $\Delta[Sr]_i$ are shown in Fig. 9 *A*. Peak free strontium levels are 1.58 times larger than calcium levels, and they decay ~6 times more slowly (a half-decay time of 32 ± 1 ms for calcium, compared to 189 ± 18 ms for strontium).

We were concerned that stimulus-evoked changes in magnesium might contribute to the fluorescence transients

FIGURE 6 Elimination of magnesium green calcium contamination using EGTA in the external solution. (*A, B*) Peak $\Delta F/F$ measurements during the experiment and average traces. (*A*) Average $\Delta F/F$ traces corresponding to treatments in (*B*). As in Fig. 5, EGTA-AM application speeds the decay in $Ca_e$ (*ii*), and reveals an early fast-decaying component in $Sr_e$ (*iii*), which is largely eliminated in Sr-EGTA$_e$ (*v*). (*C*) Transients in $Sr_e$ and Sr-EGTA$_e$, enlarged and overlaid. The early fast component in $Sr_e$ is greatly reduced by EGTA in the external solution. The difference between these two traces is plotted in *D* (*noisy trace*), with the calcium transient normalized to the same peak height and overlaid for comparison (*dotted line*).
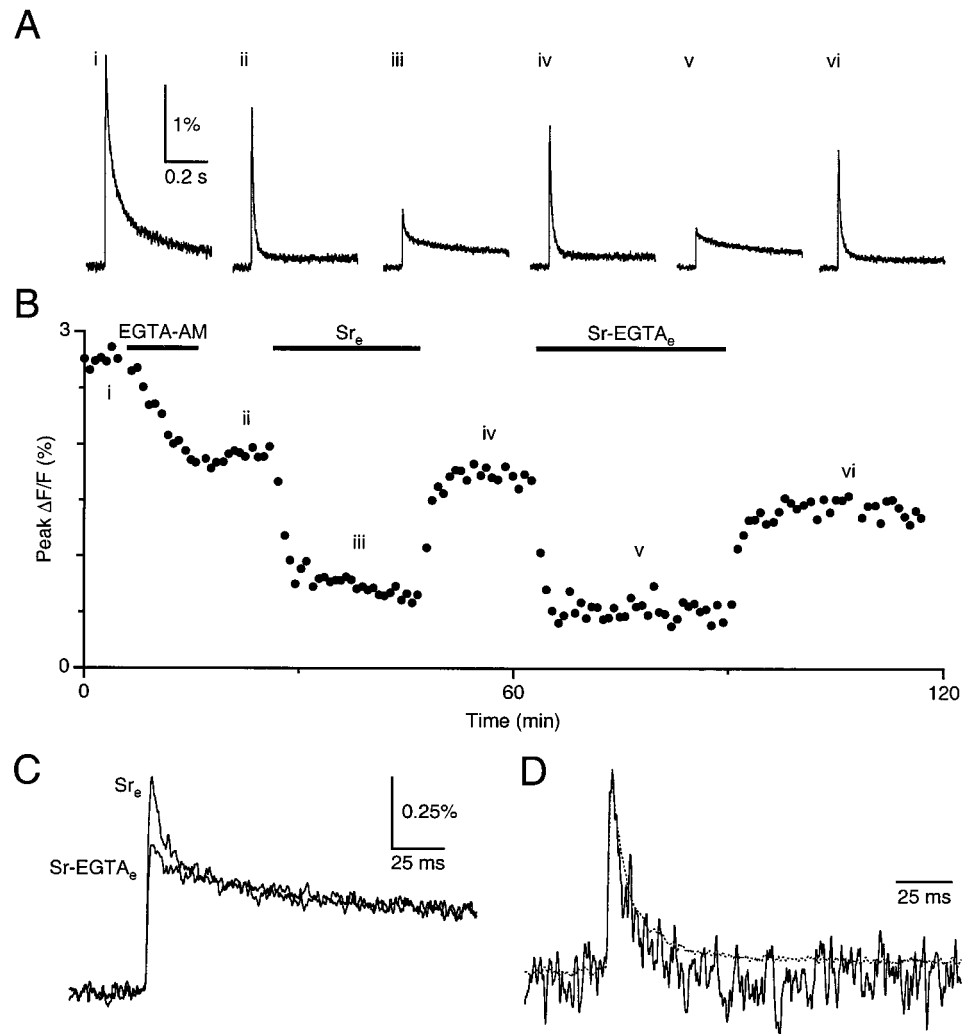
measured with magnesium green, which binds magnesium with a dissociation constant of 1 mM. We therefore repeated these experiments with fura-2FF (Fig. 9 *B*), which is insensitive to magnesium (see Methods). Estimates of peak $\Delta[Sr]_i$ were slightly larger for fura-2FF (1.89 times that of the calcium transient). The time courses of the signals had a half-decay time of $46 \pm 2$ ms ($n = 6$) in $Ca_e$, and $179 \pm 13$ ms in Sr-EGTA$_e$, similar to those measured using magnesium green (Fig. 9 *C*). The similarity of the magnesium green and the fura-2FF signals indicates that magnesium does not contribute significantly to the fluorescence transients measured with magnesium green.

## The effect of Sr-EGTA$_e$ on neurotransmitter release

To allow us to make a direct comparison between release rates and presynaptic divalent levels for calcium and strontium, we repeated the electrophysiological experiments of Fig. 2 in Sr-EGTA$_e$ to eliminate contamination by calcium (Fig. 10 *A*). Qualitatively, the results were similar to those obtained in $Sr_e$ (Fig. 2) with a drop in amplitude and

slowing of the time course of the EPSC (Fig. 10 *A, inset*). On average, peak EPSCs were smaller in Sr-EGTA$_e$ ($8.8 \pm 0.9\%$ of control, $n = 5$) than in $Sr_e$ ($13.5 \pm 1.4\%$ of control, $n = 7$).

We also tested the effect of Sr-EGTA$_e$ on fiber excitability, and on the amplitude and frequency of mEPSCs. As shown in Fig. 10 *B*, the amplitude of the presynaptic volley was virtually identical in Sr-EGTA$_e$ and in $Ca_e$. This indicates that differences in the number of fibers excited does not contribute to differences in the EPSCs evoked in Sr-EGTA$_e$ and in $Ca_e$. Additionally, we found that the amplitude distribution, average size, and time course of spontaneous mEPSCs were the same in Sr-EGTA$_e$ and $Ca_e$ (Fig. 10 *C*). Thus, changes in the average mEPSC time course or amplitude do not contribute to differences in the evoked EPSCs in Sr-EGTA$_e$ and in $Ca_e$. The mEPSC frequency was elevated ~50% in the presence of Sr-EGTA$_e$. At present we do not know why the mEPSC frequency increases. We were unable to detect any change in resting fluorescence levels with any of the indicators in the presence of Sr-EGTA$_e$, indicating that it is unlikely to be a consequence of changes in resting divalent levels, although it is difficult to defini-
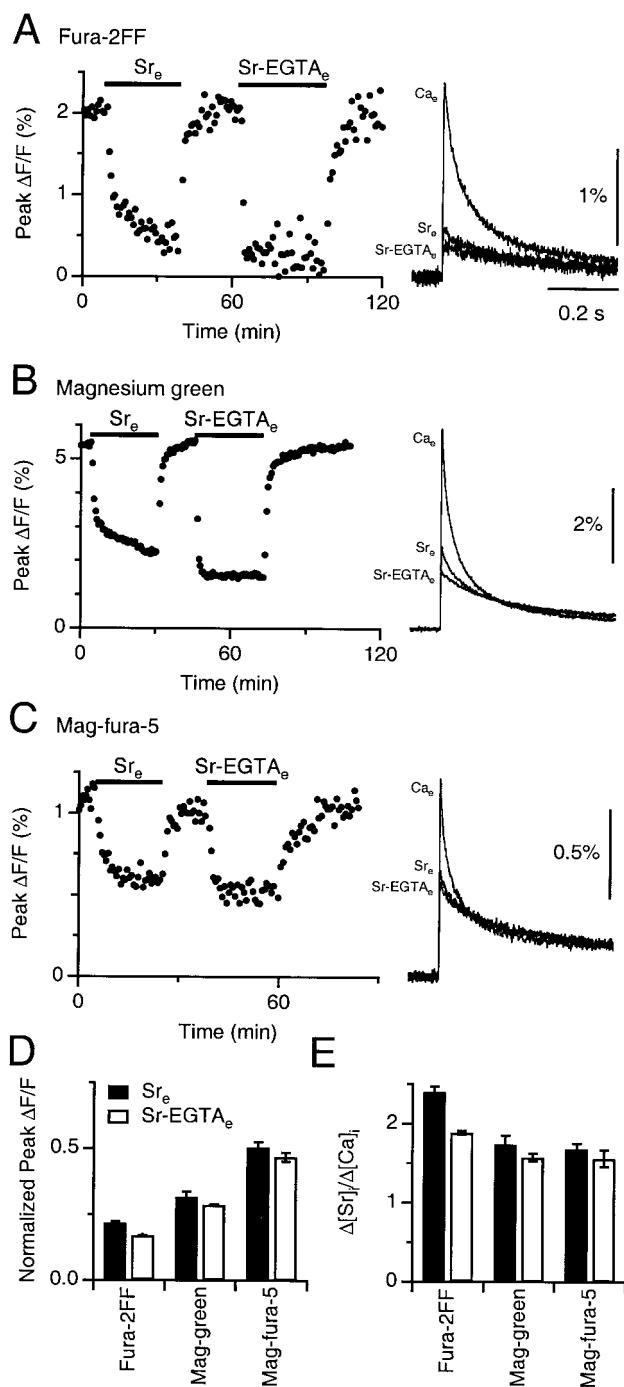
FIGURE 7    Effect of $Sr_e$ and Sr-EGTA$_e$ on fluorescence transients measured with fura-2FF (*A*), magnesium green (*B*), and mag-fura-5 (*C*). *Left column:* Peak $\Delta F/F$ measurements in response to parallel fiber stimulation. *Right column:* Average traces for $Ca_e$, $Sr_e$, and Sr-EGTA$_e$ overlaid. (*D*) Peak $\Delta F/F$ transients in $Sr_e$ and Sr-EGTA$_e$, normalized by the $Ca_e$ peak $\Delta F/F$ for the three low-affinity indicators. Peak levels are all lower in Sr-EGTA$_e$ compared to $Sr_e$. Points are averages of 4–9 experiments ±SE. (*E*) Peak free strontium levels relative to calcium for the three low-affinity indicators. These values are calculated from (*D*), using Eq. 1.

tively rule out this possibility. The onset of the frequency increase was slower than the effect on evoked synaptic current. This suggests that changes in release in Sr-EGTA$_e$

are primarily a consequence of the change in the stimulus-evoked divalent transient.

A comparison of the EPSCs measured in $Ca_e$ with those measured in Sr-EGTA$_e$ reveals that although the peak amplitude is smaller in Sr-EGTA$_e$, 20 ms after stimulation the synaptic current is larger in Sr-EGTA$_e$ (Fig. 10 *D*). Furthermore, EPSCs recorded in Sr-EGTA$_e$ and in $Ca_e$ each have a fast and a slow component. The fast component is much more prominent in $Ca_e$, while the slow component is more prominent in Sr-EGTA$_e$. Because the mEPSC time courses are the same in Sr-EGTA$_e$ and in $Ca_e$, the average evoked EPSCs can be used to compare the relative release rate in Sr-EGTA$_e$ and in $Ca_e$ for times long compared to the duration of the mEPSC. Thus, during this slow decay phase the release rate is ~2–4 times as large in Sr-EGTA$_e$ as in $Ca_e$. These findings are similar to those described at hippocampal synapses, which gave rise to the hypothesis that the two components of release correspond to high- and low-affinity calcium binding sites, with strontium preferentially activating the high-affinity site (Goda and Stevens, 1994). However, the interpretation changes when we consider presynaptic strontium and calcium levels, as described below.

## Release as a function of presynaptic strontium and calcium levels

Average presynaptic free divalent levels ($\Delta[Ca]_i$ and $\Delta[Sr]_i$) measured using magnesium green, and EPSCs measured in $Ca_e$ and Sr-EGTA$_e$, are summarized in Fig. 11 *A*. Release can be described as a function of the divalent concentration (Fig. 11 *B*). The shape of the dependence in Fig. 11 *B* indicates that in $Ca_e$, the release of neurotransmitter consists of two components, as reported previously (Goda and Stevens, 1994; Atluri and Regehr, 1998). The first component covers the first 40 ms after stimulation. During this period, calcium drops to ~50% of peak levels and the EPSC drops below 1% of peak values, indicating that release is steeply dependent on calcium. A more quantitative analysis of the release rate during the first component is complicated by two factors: 1) the kinetics of the calcium-dependent release process, and 2) the kinetics of the mEPSC (Katz and Miledi, 1964; Diamond and Jahr, 1995; Isaacson and Walmsley, 1995; Atluri and Regehr, 1996, 1998; Bertram et al., 1996). However, there is little doubt that calcium is more effective than strontium during this phase of release, in agreement with previous conclusions (Goda and Stevens, 1994) that did not consider differences in intracellular strontium and calcium transients.

In considering the second component of release, which corresponds to the period 40 ms after stimulation, we reach a different conclusion from previous reports. As calcium levels drop from 50% to ~7% of peak levels, the EPSC drops from ~1% to 0.1% of peak levels, indicating that release is less steeply dependent on calcium. The second component is not subject to the two complicating factors
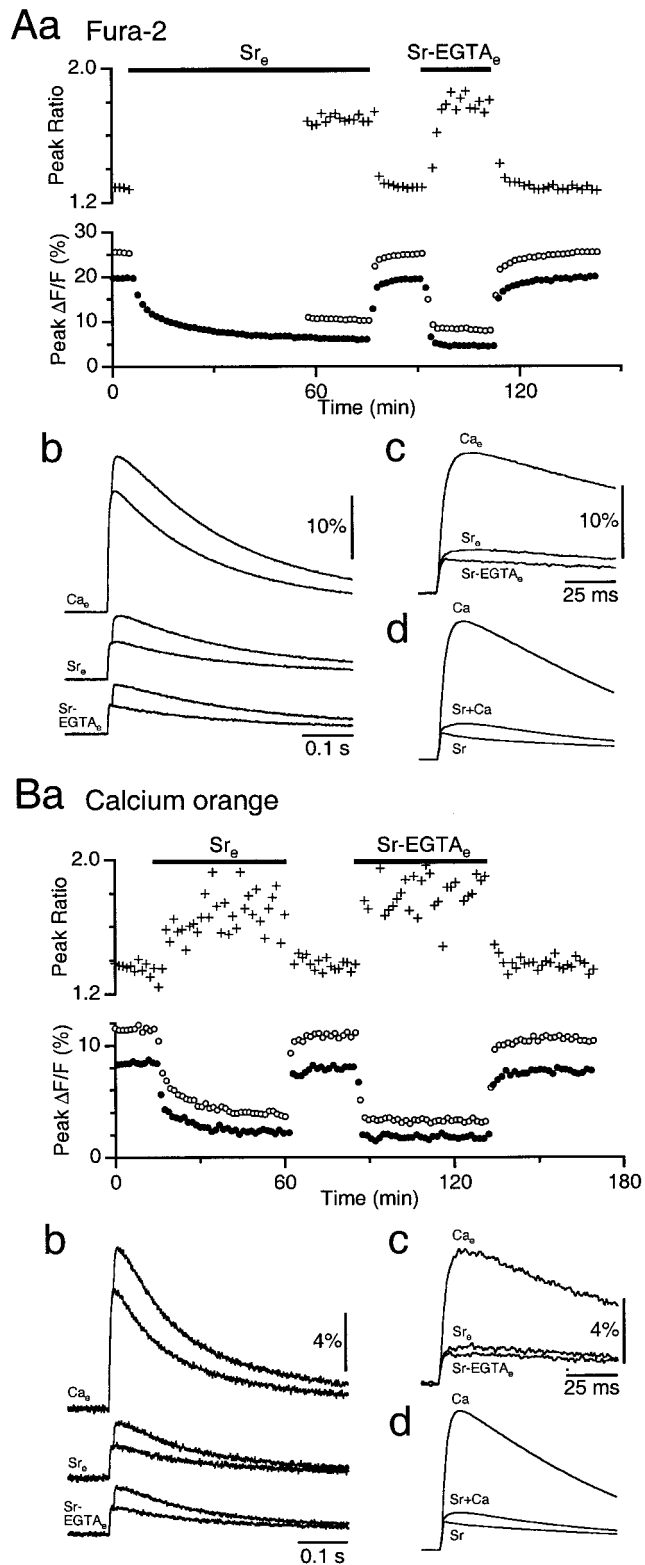
just mentioned, because divalents are probably in equilibrium with the release process, and it takes place on a time scale much longer than the mEPSC. Therefore, the time course of the evoked EPSC provides a good measure of the time course of release, and it is possible to estimate the relative affinities for strontium and calcium (Atluri and Regehr, 1998). From Fig. 11 *B* we estimate that this component of release is 2–4 times more sensitive to calcium than to strontium. Thus it appears that strontium drives both components of release less effectively than does calcium.

## DISCUSSION

To better understand the effect of strontium on the amplitude and time course of synaptic release, we measured presynaptic strontium levels in response to axonal stimulation. We found that after single stimuli, residual free strontium reaches ~1.7 times higher peak levels, and that it decays much more slowly than calcium. Release in strontium, as in calcium, showed two components, with one more steeply dependent on divalent levels than the other. Strontium is less effective than calcium at evoking release through either of these components; thus, the higher concentration of strontium and its slower extrusion from the presynaptic terminal appear to be two important factors in the prolonged time course of release in strontium.

## Measurement of presynaptic strontium

We used a range of low- and high-affinity fluorescent indicators that gave consistent results. The low-affinity indicators were most effective for measuring the time course and amplitude of intracellular residual free strontium levels ($\Delta[Sr]_i$), as previous work has found for calcium ($\Delta[Ca]_i$) (Konishi et al., 1991; Regehr and Atluri, 1995; Atluri and Regehr, 1996; Feller et al., 1996; Zhao et al., 1996). We could account for the high-affinity indicator $\Delta F/F$ signals using a model with reasonable parameters, derived from low-affinity indicator measurements.

We also found that loading presynaptic terminals with EGTA-AM is a useful approach for discriminating calcium from strontium signals. Application of EGTA-AM accelerates the decay of $\Delta[Ca]_i$ due to the slow on-rate of EGTA (Atluri and Regehr, 1996). Because EGTA has a 300-fold higher affinity for calcium over strontium, $\Delta[Sr]_i$ is not significantly affected unless high concentrations of EGTA-AM are applied. This allowed us to separate a rapidly decaying component due to calcium from a slowly decaying component due to strontium. We found that even in a nominally calcium-free bathing solution, small amounts of contaminating calcium (<10 $\mu$M) led to measurably

FIGURE 8 Effect of $Sr_e$ and Sr-EGTA$_e$ on fluorescence transients measured with fura-2 (*A*) and calcium orange (*B*). (*a*) Peak $\Delta F/F$ measurements in response to single (*filled circles*) and double (*open circles*) stimulation, and the ratio of double- to single-peak height (+). In this experiment, double pulses were not delivered during wash-in of $Sr_e$ to reduce bleaching. (*b*) Average traces for single- and double-pulse stimuli in Ca$_e$, Sr$_e$, and Sr-EGTA$_e$. (*c*) Average traces for single pulses from *b* overlaid. (*d*) Responses of a computational model to calcium influx (Ca), to strontium influx with contaminating calcium (Sr + Ca), and to strontium influx (Sr). Parameters (see Methods) were determined by fitting data using low-affinity indicators, and then substituting the kinetics and binding affinity of fura-2 or calcium orange.
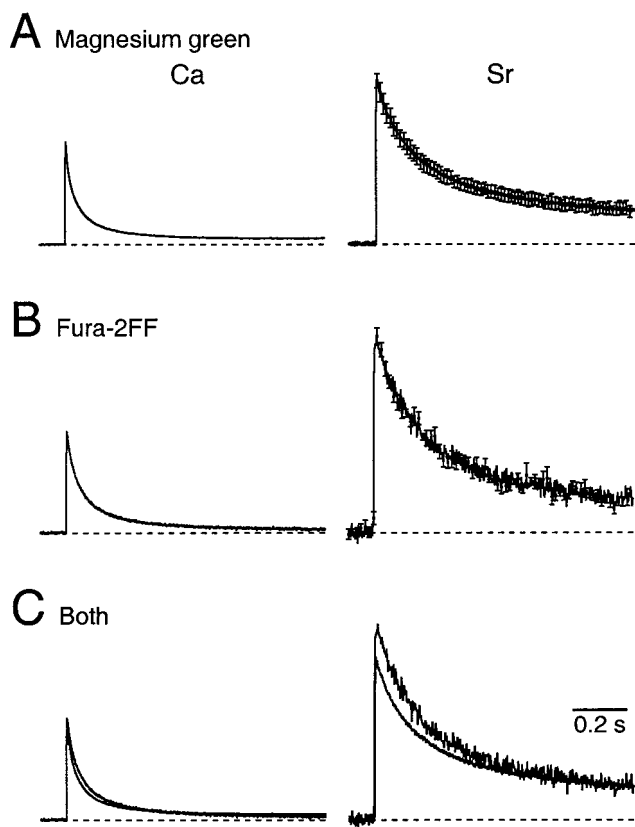
## A Magnesium green

Ca              Sr

## B Fura-2FF

## C Both

0.2 s

FIGURE 9   Residual presynaptic calcium (*left*) and strontium (*right*) levels measured using magnesium green (*A*) and fura-2FF (*B*). Data for both indicators are overlaid in (*C*). Traces are averages from five experiments for magnesium green and six for fura-2FF, with error bars shown only for strontium in (*A*) and (*B*), because error bars in calcium are hidden in the line thickness. Error bars are means ± SE. Averages traces were computed after aligning the transients by the time of fastest rise, and normalizing $\Delta[Ca]_i$ and $\Delta[Sr]_i$ from the same experiment by the peak height of the $\Delta F/F$ transient in $Ca_e$.

higher $\Delta F/F$ signals. To obtain a clean signal of free strontium levels, we had to use EGTA buffering externally. We further found that this solution had the experimental advantages of fast wash-in and wash-out.

### Differences in free strontium peak amplitude and decay

Our measurements allow us to make a preliminary description of the mechanisms that control the amplitude and time course of strontium levels in presynaptic terminals. In the simplest case of one high-capacity endogenous buffer at equilibrium, the relative peak free divalent levels are given by

$$\frac{(\Delta[Sr]_i)_{peak}}{(\Delta[Ca]_i)_{peak}} \approx \left(\frac{\Delta[Sr]_{total}}{\Delta[Ca]_{total}}\right)\left(\frac{K_{Sr}}{K_{Ca}}\right), \qquad (2)$$

where $\Delta[Sr]_{total}$ and $\Delta[Ca]_{total}$ are the changes in total divalent concentrations in the presynaptic terminal due to calcium channel opening, and $K_{Sr}$ and $K_{Ca}$ are the dissoci-

ation constants of the endogenous buffer for strontium and calcium, respectively. We found that $(\Delta[Sr]_i)_{peak}$ is 1.6–1.9 times larger than $(\Delta[Ca]_i)_{peak}$ following single stimuli. As shown in Eq. 2, this difference results from relative differences in both influx and buffering.

Divalent influx is a function of the action potential waveform and the kinetics and permeabilities of calcium channels. Because the action potential is unaffected by replacement of calcium with strontium in the bathing solution (Fig. 10 *B*), alterations in influx appear to arise solely from permeability differences. Estimation of the relative strontium and calcium permeability is complicated by the fact that several calcium channel types are present in granule cell terminals, including ω-conotoxin-GVIA-sensitive (N-type, 27%) and ω-Aga-IVA-sensitive (P/Q-type, 50%), plus a toxin-insensitive component (23%) (Mintz et al., 1995). The relative permeability of all of these channel types for strontium has not been well characterized. It is known that the permeability of strontium relative to calcium for expressed N-type calcium channels is 1–1.2 (Mangoni et al., 1997; Wakamori et al., 1998).

Returning to Eq. 2, and using the permeability ratio for expressed N-type channels for $\Delta[Sr]_{total}/\Delta[Ca]_{total}$, we estimate $K_{Sr}/K_{Ca}$ to be 1.3 to 1.9. Thus, a combination of slightly greater influx of strontium and lower binding affinity of the endogenous buffer results in higher peak $\Delta[Sr]_i$. More refined estimates of the contribution of differential influx and differential buffering await direct measurement of strontium permeability through the calcium channels present at granule cell terminals.

We determined that $\Delta[Sr]_i$ decays more slowly than $\Delta[Ca]_i$. The decay of free divalent levels in the presynaptic terminal is controlled by the interaction between the endogenous buffer and extrusion via the Ca-ATPase pump and the Na/Ca exchanger. This interaction is complex for normal calcium extrusion (Regehr, 1997), but if we approximate extrusion using a single Michaelis-Menten process well below saturation (Sala and Hernandez-Cruz, 1990), then free divalent levels decay exponentially with a time constant of $\tau_{Sr}$ for strontium and $\tau_{Ca}$ for calcium:

$$\frac{\tau_{Sr}}{\tau_{Ca}} \approx \frac{(V_{max}/K_p)_{Ca}}{(V_{max}/K_p)_{Sr}} \frac{K_{Ca}}{K_{Sr}}, \qquad (3)$$

where $V_{max}$ is the pump's maximum efflux rate and $K_p$ is the pump's half-maximal concentration (Tank et al., 1995). Although the actual decay of calcium we observe is not exponential, Eq. 3 provides a framework for understanding the factors that could lead to differences in decay for strontium and calcium; the decay is faster if extrusion is faster, and slower if the dissociation constant of the endogenous buffer for the divalent decreases. We found the half-decay times of strontium to be 190 ms and calcium to be 32 ms, thus we estimate $\tau_{Sr}/\tau_{Ca}$ to be ~6. As described above, we estimate $K_{Sr}/K_{Ca}$ to be 1.3–1.9. The lower capacity of the endogenous buffer for strontium would tend to speed up the decay of strontium relative to calcium. To account for the
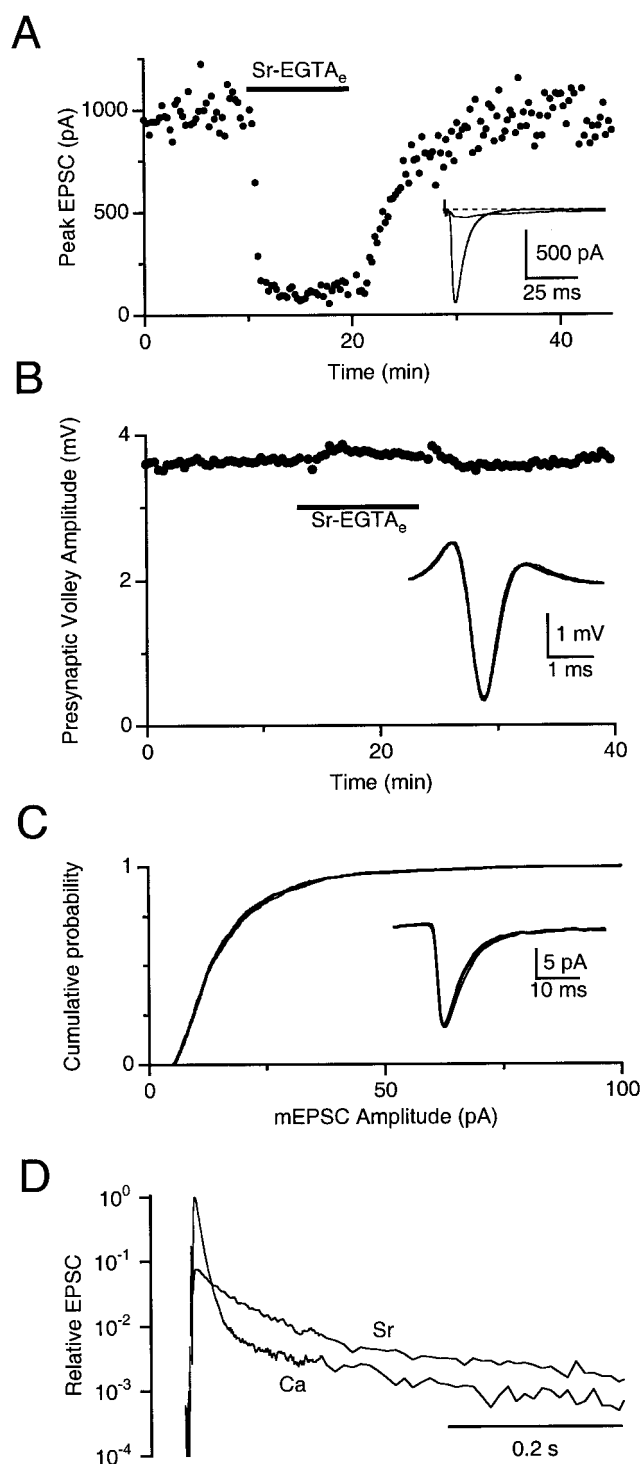
## A



## B



## C



## D



FIGURE 10   Effect of Sr-EGTA$_e$ on synaptic release. (*A*) EPSC peak amplitude drops when the external solution is changed from Ca$_e$ to Sr-EGTA$_e$. Each circle represents the peak of the EPSC following single stimuli. *Inset:* Average EPSCs in Ca$_e$ and Sr-EGTA$_e$ overlaid. (*B*) Presynaptic volley is minimally affected by Sr-EGTA$_e$. Each circle represents the peak-to-peak height of the field potential recorded in the molecular layer in response to stimulation. *Inset:* Average traces recorded in Ca$_e$ and Sr-EGTA$_e$ overlaid (Ca$_e$ trace shifted earlier by 0.2 ms). (*C*) Cumulative probability distribution of mEPSC amplitude measured in Sr-EGTA$_e$ and Ca$_e$. *Inset* shows superimposed average mEPSC measured in Sr-EGTA$_e$ and Ca$_e$. (*D*) Semilog plot of average EPSCs in Ca$_e$ ($n = 10$ cells) and Sr-EGTA$_e$ ($n = 4$ cells). Average traces were computed after aligning the
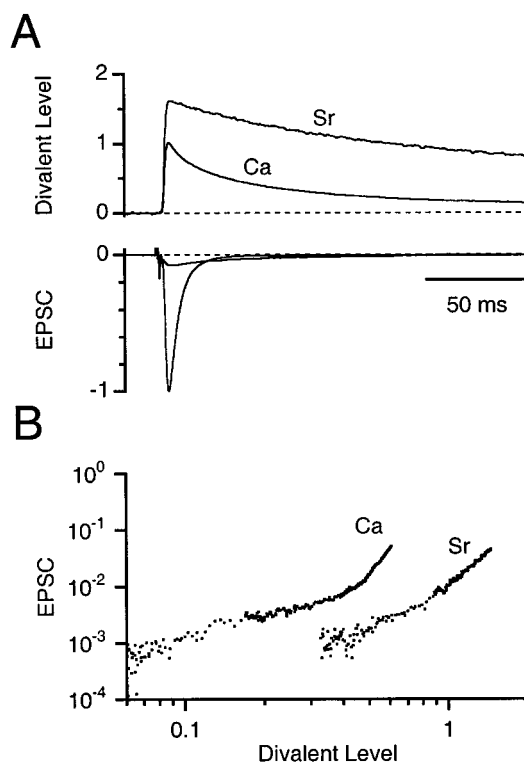
## A



## B



FIGURE 11   Synaptic release as a function of strontium and calcium. All strontium measurements were done in Sr-EGTA$_e$. (*A*) Average EPSC and fluorescence transients. *Top graph:* Fluorescence transients measured using magnesium green, from Fig. 9 (*A*). *Bottom graph:* Average EPSCs, from Fig. 10 (*D*). (*B*) EPSC as a function of $\Delta[Sr]_i$ and $\Delta[Ca]_i$, using data in (*A*), starting 20 ms after the peak and continuing for 1 s.

sixfold increase in decay time, extrusion must be 8 to 11 times slower for strontium than for calcium.

The time course and amplitude of free strontium levels are expected to vary at different presynaptic terminals. The calcium channels, endogenous buffers, and extrusion mechanisms can vary greatly for different terminals. Furthermore, because all these components evolved to regulate calcium and not strontium, their relative efficacy in strontium is difficult to estimate a priori. Therefore, for other synapses, it is important to individually assess their peak strontium levels and rates of decay.

## Strontium and release

Our results show that peak free strontium levels following single stimuli are higher than calcium levels and decay more slowly. When we compare free divalent levels with release, we observe two components (Fig. 11): one steeply dependent on divalent levels, and one more linearly dependent on divalent levels. For all measured concentrations of free

transients by the time of fastest rise, and normalizing calcium- and strontium-induced EPSCs from the same experiment by the peak height of the EPSC measured in Ca$_e$.

divalents, the release rate in strontium is lower than the release rate in calcium. The simplest explanation for this is that the affinities of both calcium-dependent components are lower for strontium than for calcium. The large asynchronous component, which is the hallmark of strontium's effects on release, can be accounted for by the higher peak levels and slower removal of strontium from the presynaptic terminal.

One important implication of the relationship between presynaptic free strontium levels and release is that greater sensitivity to strontium may not serve to identify molecules involved in asynchronous release. Previous work did not measure presynaptic divalent levels, and therefore assumed that strontium decays with the same time course as calcium, leading to the conclusion that asynchronous release was more sensitive to strontium than to calcium (Goda and Stevens, 1994). We found, however, that strontium transients are larger and slower than calcium transients, implying that strontium is less effective than calcium at driving the slow component of release. This will have to be taken into account in attempts to use strontium binding affinity to identify high-affinity calcium sensors involved in release (Li et al., 1995).

## REFERENCES

Abdul-Ghani, M. A., T. A. Valiante, and P. S. Pennefather. 1996. $Sr^{2+}$ and quantal events at excitatory synapses between mouse hippocampal neurons in culture. *J. Physiol.* 495:113–125.

Adler, E. M., G. J. Augustine, S. N. Duffy, and M. P. Charlton. 1991. Alien intracellular calcium chelators attenuate neurotransmitter release at the squid giant synapse. *J. Neurosci.* 11:1496–1507.

Atluri, P. P., and W. G. Regehr. 1996. Determinants of the time course of facilitation at the granule cell to Purkinje cell synapse. *J. Neurosci.* 16:5661–5671.

Atluri, P. P., and W. G. Regehr. 1998. Delayed release of neurotransmission from cerebellar granule cells. *J. Neurosci.* 18:8214–8227.

Augustine, G. J., and R. Eckert. 1984. Divalent cations differentially support transmitter release at the squid giant synapse. *J. Physiol. (Lond.).* 346:257–271.

Bain, A. I., and D. M. J. Quastel. 1992. Quantal transmitter release mediated by strontium at the mouse motor nerve terminal. *J. Physiol.* 450:63–87.

Behrends, J. C., and G. ten Bruggencate. 1998. Changes in quantal size distributions upon experimental variations in the probability of release at striatal inhibitory synapses. *J. Neurophysiol.* 79:2999–3011.

Bers, D. M. 1982. A simple method for the accurate determination of free [Ca] in Ca-EGTA solutions. *Am. J. Physiol.* 242:C404–C408.

Bertram, R., A. Sherman, and E. F. Stanley. 1996. Single-domain/bound calcium hypothesis of transmitter release and facilitation. *J. Neurophysiol.* 75:1919–1931.

Choi, S., and D. M. Lovinger. 1997. Decreased frequency but not amplitude of quantal synaptic responses associated with expression of corticostriatal long-term depression. *J. Neurosci.* 17:8613–8620.

Delaney, K. R., and D. W. Tank. 1994. A quantitative measurement of the dependence of short-term synaptic enhancement on presynaptic residual calcium. *J. Neurosci.* 14:5885–5902.

Delaney, K. R., R. S. Zucker, and D. W. Tank. 1989. Calcium in motor nerve terminals associated with posttetanic potentiation. *J. Neurosci.* 9:3558–3567.

Diamond, J. S., and C. E. Jahr. 1995. Asynchronous release of synaptic vesicles determines the time course of the AMPA receptor-mediated EPSC. *Neuron.* 15:1097–1107.

Dodge, F. A. J., R. Miledi, and R. Rahamimoff. 1969. Strontium and quantal release of transmitter at the neuromuscular junction. *J. Physiol.* 200:267–283.

Feller, M. B., K. R. Delaney, and D. W. Tank. 1996. Presynaptic calcium dynamics at the frog retinotectal synapse. *J. Neurophysiol.* 76:381–400.

Fujimori, T., and W. P. Jencks. 1992a. Binding of two $Sr^{2+}$ ions changes the chemical specificities for phosphorylation of the sarcoplasmic reticulum calcium ATPase through a stepwise mechanism. *J. Biol. Chem.* 267:18475–18487.

Fujimori, T., and W. P. Jencks. 1992b. The kinetics for the phosphoryl transfer steps of the sarcoplasmic reticulum calcium ATPase are the same with strontium and with calcium bound to the transport sites. *J. Biol. Chem.* 267:18466–18474.

Goda, Y., and C. F. Stevens. 1994. Two components of transmitter release at a central synapse. *Proc. Natl. Acad. Sci. USA.* 91:12942–12946.

Graf, E., A. K. Verma, J. P. Gorski, G. Lopaschuk, V. Niggli, M. Zurini, E. Carafoli, and J. T. Penniston. 1982. Molecular properties of calcium-pumping ATPase from human erythrocytes. *Biochemistry.* 21:4511–4516.

Grynkiewicz, G., M. Poenie, and R. Y. Tsien. 1985. A new generation of $Ca^{2+}$ indicators with greatly improved fluorescence properties. *J. Biol. Chem.* 260:3440–3450.

Hagiwara, S., and H. Ohmori. 1982. Studies of calcium channels in rat clonal pituitary cells with patch electrode voltage clamp. *J. Physiol.* 331:231–252.

Herrington, J., and R. J. Bookman. 1995. Pulse Control V4.5: IGOR XOPs for Patch Clamp Data Acquisition. University of Miami, Miami, FL.

Hess, P., J. B. Lansman, and R. W. Tsien. 1986. Calcium channel selectivity for divalent and monovalent cations. *J. Gen. Physiol.* 88:293–319.

Isaacson, J. S., and B. Walmsley. 1995. Counting quanta: direct measurements of transmitter release at a central synapse. *Neuron.* 15:875–884.

Kamiya, H., and R. S. Zucker. 1994. Residual $Ca^{2+}$ and short-term synaptic plasticity. *Nature.* 371:603–606.

Katz, B., and R. Miledi. 1964. The measurement of synaptic delay, and the time course of acetylcholine release at the neuromuscular junction. *Proc. R. Soc. Lond. B.* 161:483–495.

Konishi, M., S. Hollingworth, A. B. Harkins, and S. M. Baylor. 1991. Myoplasmic calcium transients in intact frog skeletal muscle fibers monitored with the fluorescent indicator furaptra. *J. Gen. Physiol.* 97:271–301.

Lévénès, C., H. Daniel, P. Soubrié, and F. Crépel. 1998. Cannabinoids decrease excitatory synaptic transmission and impair long-term depression in rat cerebellar Purkinje cells. *J. Physiol.* 510:867–879.

Li, C., B. A. Davletov, and T. C. Südhof. 1995. Distinct $Ca^{2+}$ and $Sr^{2+}$ binding properties of synaptotagmins. Definition of candidate $Ca^{2+}$ sensors for the fast and slow components of neurotransmitter release. *J. Biol. Chem.* 270:24898–24902.

London, R. E., L. A. Levy, and E. Murphy. 1996. Fluorescent intracellular calcium indicators. US Patent 5,516,911.

Mangoni, M. E., T. Cens, C. Dalle, J. Nargeot, and P. Charnet. 1997. Characterisation of alpha 1A $Ba^{2+}$, $Sr^{2+}$ and $Ca^{2+}$ currents recorded with the ancillary beta 1–4 subunits. *Receptors and Channels.* 5:1–14.

Martell, A. E., and R. M. Smith. 1974. Critical Stability Constants, Vol. 1. Plenum Press, New York.

Meiri, U., and R. Rahamimoff. 1971. Activation of transmitter release by strontium and calcium ions at the neuromuscular junction. *J. Physiol.* 215:709–726.

Mellow, A. M., B. D. Perry, and E. M. Silinsky. 1982. Effects of calcium and strontium in the process of acetylcholine release from motor nerve endings. *J. Physiol.* 328:547–562.

Mermier, P., and W. Hasselbach. 1976. Comparison between strontium and calcium uptake by the fragmented sarcoplasmic reticulum. *Eur. J. Biochem.* 69:79–86.

Miledi, R. 1966. Strontium as a substitute for calcium in the process of transmitter release at the neuromuscular junction. *Nature.* 212:1233–1234.

Miller, D. J., and G. L. Smith. 1984. EGTA purity and the buffering of calcium ions in physiological solutions. *Am. J. Physiol.* 246:C160–C166.

Mintz, I. M., B. L. Sabatini, and W. G. Regehr. 1995. Calcium control of transmitter release at a cerebellar synapse. *Neuron.* 15:675–688.

Moisescu, D. G., and H. Pusch. 1975. A pH-metric method for the determination of the relative concentration of calcium to EGTA. *Pflügers Arch.* 355(Suppl.):R122.

Morishita, W., and B. E. Alger. 1997. $Sr^{2+}$ supports depolarization-induced suppression of inhibition and provides new evidence for a presynaptic expression mechanism in rat hippocampal slices. *J. Physiol.* 505:307–317.

Murray, R. K., and M. I. Kotlikoff. 1991. Receptor-activated calcium influx in human airway smooth muscle cells. *J. Physiol.* 435:123–144.

Oliet, S. H. R., R. C. Malenka, and R. A. Nicoll. 1996. Bidirectional control of quantal size by synaptic activity in the hippocampus. *Science.* 271:1294–1297.

Otis, T. S., M. P. Kavanaugh, and C. E. Jahr. 1997. Postsynaptic glutamate transport at the climbing fiber-Purkinje cell synapse. *Science.* 277:1515–1518.

Palay, S. L., and V. Chan-Palay. 1974. Cerebellar Cortex. Springer-Verlag, New York.

Rasgado-Flores, H., S. Sanchez-Armass, M. P. Blaustein, and D. A. Nachshen. 1987. Strontium, barium, and manganese metabolism in isolated presynaptic nerve terminals. *Am. J. Physiol.* 252:C604–C610.

Regehr, W. G. 1997. Interplay between sodium and calcium dynamics in granule cell presynaptic terminals. *Biophys. J.* 72:2476–2488.

Regehr, W. G., and P. P. Atluri. 1995. Calcium transients in cerebellar granule cell presynaptic terminals. *Biophys. J.* 68:2156–2170.

Regehr, W. G., and D. W. Tank. 1991. Selective fura-2 loading of presynaptic terminals and nerve cell processes by local perfusion in mammalian brain slice. *J. Neurosci. Meth.* 37:111–119.

Sabatini, B. L., and W. G. Regehr. 1995. Detecting changes in calcium influx which contribute to synaptic modulation in mammalian brain slice. *Neuropharmacology.* 34:1453–1467.

Sage, S. O., J. E. Merritt, T. J. Hallam, and T. J. Rink. 1989. Receptor-mediated calcium entry in fura-2-loaded human platelets stimulated with ADP and thrombin. *Biochem. J.* 258:923–926.

Sala, F., and A. Hernandez-Cruz. 1990. Calcium diffusion modeling in a spherical neuron. *Biophys. J.* 57:313–324.

Smith, P. D., G. W. Liesegang, R. L. Berger, G. Czerlinski, and R. J. Podolsky. 1984. A stopped-flow investigation of calcium ion binding by ethylene glycol bis(beta-aminoethyl ether)-*N*,*N*′-tetraacetic acid. *Anal. Biochem.* 143:188–195.

Stanley, E. F. 1986. Decline in calcium cooperativity as the basis of facilitation at the squid giant synapse. *J. Neurosci.* 6:782–789.

Swandulla, D., M. Hans, K. Zipser, and G. J. Augustine. 1991. Role of residual calcium in synaptic depression and posttetanic potentiation: fast and slow calcium signaling in nerve terminals. *Neuron.* 7:915–926.

Tank, D. W., W. G. Regehr, and K. R. Delaney. 1995. A quantitative analysis of presynaptic calcium dynamics that contribute to short-term enhancement. *J. Neurosci.* 15:7940–7952.

Tsien, R. Y. 1980. New calcium indicators and buffers with high selectivity against magnesium and protons: design, synthesis, and properties of prototype structures. *Biochemistry.* 19:2396–2404.

Tsien, R. Y. 1981. A non-disruptive technique for loading calcium buffers and indicators into cells. *Nature.* 290:527–528.

Tsien, R., and T. Pozzan. 1989. Measurement of cytosolic free $Ca^{2+}$ with Quin2. *Methods Enzymol.* 172:230–262.

Vega, M. T., C. Villalobos, B. Garrido, L. Gandía, O. Bulbena, J. García-Sancho, A. G. García, and A. R. Artalejo. 1994. Permeation by zinc of bovine chromaffin cell calcium channels: relevance to secretion. *Pflügers Arch.* 429:231–239.

Wakamori, M., M. Strobeck, T. Niidome, T. Teramoto, K. Imoto, and Y. Mori. 1998. Functional characterization of ion permeation pathway in the N-type $Ca^{2+}$ channel. *J. Neurophysiol.* 79:622–634.

Zhao, M., S. Hollingworth, and S. M. Baylor. 1996. Properties of tri and tetracarboxylate $Ca^{2+}$ indicators in frog skeletal muscle fibers. *Biophys. J.* 70:896–916.